

A novel beta-catenin homologue from the earthworm *Eisenia andrei*: Identification and characterization during embryonic development, segment regeneration, and immune response

Kornélia Bodó^{a,1}, Ákos Boros^b, Chayeen Brotzki da Costa^a, Gréta Tolnai^a, Éva Rumpler^{c,2}, Zoltán László^b, György Nagyri^{d,e}, Péter Németh^a, Peter Kille^f, László Molnár^g, Péter Engelmann^{a,*}

^a Department of Immunology and Biotechnology, Medical School, Clinical Center, University of Pécs, H-7624 Pécs, Hungary

^b Department of Medical Microbiology and Immunology, Medical School, Clinical Center, University of Pécs, H-7624 Pécs, Hungary

^c Department of Comparative Anatomy and Developmental Biology, Institute of Biology, Faculty of Sciences, University of Pécs, H-7624 Pécs, Hungary

^d Department of Neurobiology, Institute of Biology, Faculty of Sciences, University of Pécs, H-7624 Pécs, Hungary

^e Department of Animal Biotechnology, Institute of Genetics and Biotechnology, Hungarian University of Agriculture and Life Sciences, Szent-Györgyi Albert Street 4, H-2100 Gödöllő, Hungary

^f School of Biosciences, Cardiff University, Cardiff CF10 3AX, UK

^g Ecophysiological and Ecotoxicological Research Group, HUN-REN, Balaton Limnological Research Institute, H-8237 Tihany, Hungary

ARTICLE INFO

Keywords:

Development
Immune response
Intracellular signaling
Molecular interactions
Morphogens
Regeneration

ABSTRACT

Evolutionarily, Wnt/ β -catenin signaling is well-conserved and supports several key cell-biological processes (e.g. adhesion and proliferation). Its crucial component, β -catenin, has been described in several organisms, however, its identification and characterization are notably lacking in annelid earthworms.

Here, we report a novel β -catenin homologue from the earthworm *Eisenia andrei*, termed *Ea*- β -catenin. The full-length 3253 nt *Ea*- β -catenin mRNA includes an open reading frame of 2499 nt encoding a putative protein with 833 amino acid residues that comprise 11 classical armadillo-repeat regions. Phylogenetic analysis indicates that *Ea*- β -catenin shows strong homology with Lophotrochozoan β -catenins. Ubiquitous, but variable expressions of *Ea*- β -catenin were observed in distinct earthworm tissues. During embryogenesis, *Ea*- β -catenin mRNA gradually increased from the E1 to E4 developmental stages. Regeneration experiments revealed an inverse correlation between *Ea*- β -catenin mRNA levels and the rate of EdU⁺/PY489- β -catenin⁺ proliferating cells during the second week of the posterior blastema formation. *In vitro* exposures to poly(I:C) and zymosan significantly increased *Ea*- β -catenin mRNA levels, while small molecule Wnt-pathway modulators such as LiCl or iCRT14 increased or decreased *Ea*- β -catenin mRNA expression, and nuclear translocation of PY489- β -catenin, respectively.

These novel results pave the way for follow-up studies aimed at characterizing additional members of the Wnt/ β -catenin pathway that may be involved in embryonic and/or postembryonic development, as well as innate immunity in earthworms.

1. Introduction

During evolution, several morphogen pathways have been maintained throughout metazoan organisms. Among these pathways, the Wingless-integrated/beta-catenin (Wnt/ β -catenin) signaling is one of the most well-characterized, being conserved from sponges to mammals

[1]. It has essential and versatile functions in a variety of biological processes including ontogenesis, organogenesis, and malignant transformation [2].

The β -catenin (named armadillo in *Drosophila*) protein is the central and key nuclear effector component of the canonical Wnt-signaling pathway, exerting a critical role in the assembly of developmental and

* Corresponding author at: Department of Immunology and Biotechnology, Clinical Center, University of Pécs, Pécs H-7643, Szigeti u. 12, Hungary.
E-mail address: engelmann.peter@pte.hu (P. Engelmann).

¹ Present address: National Laboratory of Virology, Szentágotthai Research Center, University of Pécs, H-7624 Pécs, Hungary.

² Present address: Laboratory of Reproductive Neurobiology, HUN-REN Institute of Experimental Medicine, H-1083 Budapest, Hungary.

homeostatic functions. More specifically, it has a dual role, as it is also responsible for transmitting signaling events to the nucleus thus triggering transcriptional changes. Additionally, it also participates in the cytoskeletal interactions modulating cell adhesion. These functions are mirrored in its structural arrangement: β -catenin contains several (>10) centrally located, evolutionarily conserved armadillo (ARM)-repeats that are flanked by C- and N-terminal domains (CTD and NTD, respectively). Furthermore, β -catenin directly connects to E-cadherin and Adenomatous Polyposis Coli (APC) proteins through ARM repeats, thereby shaping cadherin-based adherent junctions.

ARM repeats form helices and feature a positively charged molecular groove essential for coordinating with several binding partners [2]. Interestingly, it has been shown that the CTD region is significant in intracellular signaling, while less critical during cell adhesion. Remarkably, these dual functions in the nematode *Caenorhabditis elegans* emerged in separate β -catenin orthologues (one adhesion-, two signaling specific, and one structural homologue responsible for signaling) [3,4]. These pivotal roles of β -catenin explain its strong evolutionary conservation across invertebrate and vertebrate phyla [5].

Besides embryogenesis and sex determination, in adults, β -catenin has a vital role in the maintenance of tissue homeostasis (regeneration and remodeling) and the regulation of the immune system [6]. For instance, upon injury, β -catenin is strictly linked to maintaining the body axis gradient determining head vs. tail formation in hydra or planarian regeneration [7,8]. Injury-induced Wnt/ β -catenin expression has also been reported during appendage and internal organ regeneration in diverse vertebrate models [9,10].

Beyond developmental processes, several lines of evidence prove that β -catenin is involved in the regulation of host defense not only in vertebrates but also in invertebrates [11–13]. For instance, its misregulation can result in inflammatory disorders (autoimmune and degenerative diseases) as well as cancer; more specifically, its relationship with the immune system is well established [14]. To this end, some reports suggest that β -catenin mediates interferon production and intracellular activation of dendritic cells upon viral infection [15,16], while invertebrate (crustacean and mollusk) β -catenin has been shown to control immune response upon microbial infections [12,17].

In annelids, we have relatively limited knowledge regarding the components of the Wnt/ β -catenin pathway. So far, two molecules (the frizzled receptor and β -catenin) of the pathway have been identified in the restored segments (so-called blastema) of the freshwater oligochaete annelid *Pristina leidyi* [18]. During anterior regeneration of the polychaete *Syllis gracilis*, the presumed homologues of regeneration-related genes (e.g. *Hox* genes, β -catenin, etc.) showed upregulation in association with cellular proliferation, development, and the establishment of the body axis [19].

In contrast to other invertebrate animal groups (e.g. cnidarians, flatworms, etc.) we have no information concerning the existence and function of β -catenin in terrestrial annelids, such as earthworms.

Leveraging the evolutionary conservation of the Wnt/ β -catenin signaling pathway throughout the animal kingdom, we identified the potential homologue of β -catenin in the earthworm *Eisenia andrei* (Oligochaeta, Annelida). Here, we present the molecular characterization of a novel β -catenin homologue from *E. andrei* earthworms (*Ea*- β -catenin) reporting its tissue distributions and embryonic expression profile. We then characterized its mRNA and protein expression profile during anterior and posterior segment regeneration, alongside evaluating EdU-based cell proliferation in the restored tissues. Furthermore, to test its role during the innate immune response in earthworms we measured the *Ea*- β -catenin mRNA and protein expression patterns following various *in vitro* or *in vivo* microbial stimuli. To establish the molecular partnership of *Ea*- β -catenin with the members of the Wnt/ β -catenin pathway we tested the effects of an activator and an inhibitor of this pathway on *Ea*- β -catenin mRNA expression and the cellular localization of this protein. This novel study of a β -catenin homologue in *E. andrei* further reinforces the evidence of strong conservation of this

essential signaling protein among metazoans and its indispensable role from embryonic and postembryonic development to innate immune response.

2. Materials and methods

2.1. Earthworm husbandry

Clitellated *Eisenia andrei* earthworms (Annelida, Oligochaeta) were maintained in breeding stocks of the Faculty of Sciences, University of Pécs. Earthworms were kept in soil containing moist compost and manure at room temperature [20]. Before coelomocytes (innate immune cells) or organ isolation, earthworm specimens were placed onto wet tissue paper for 24 h to clear their gut content (for detailed information on coelomocyte isolation, please see the Supplementary Material).

2.2. RNA isolation

Total RNA was extracted from earthworm coelomocytes and ovary as we described earlier [21] using NucleoSpin® RNA isolation kit (Macherey-Nagel GmbH, Düren, Germany) according to the manufacturer's protocol. After RNA elution, the purity and concentration of samples were determined by NanoDrop at 260 nm and RNA samples were stored at -80°C .

2.3. RT-PCR, 3' and 5' rapid amplification of cDNA ends (RACE)

Reverse transcription was carried out from total RNA using High-Capacity cDNA reverse transcription kit (Thermo-Fisher Scientific, Waltham, MA, USA) according to the manufacturer's instructions. Transcriptomic assembly derived from tissue atlas from *E. fetida* (NCBI Bioproject PRJNA608692) was used for designing a set of generic primers (Bcat GenF/R, Table S1) to target β -catenin-like sequences. The *Ea*- β -catenin was detected from the cDNA of earthworm coelomocytes and ovary using the generic β -catenin primer pairs and conventional RT-PCR method. The full-length mRNA sequence of *Ea*- β -catenin was determined using a series of 3' and 5' Rapid Amplification of cDNA ends (RACE) and Dye-terminator sequencing reactions described previously [22,23]. Briefly, during the 3'/5'-RACE reactions, we used Maxima H-minus RT enzyme (Thermo-Fisher) and terminal deoxynucleotidyl transferase (TdT) enzyme with dATP (Thermo-Fisher) for reverse transcription (both 3' and 5'-RACE) and cDNA tagging (in case of 5'-RACE) reactions, respectively. For the 3'/5'-RACE PCR reactions, *Ea*- β -catenin specific reverse (5'-RACE), forward (3'-RACE) primers (Table S1), and anchored oligo dT-adapter primers (Table S1) were used in multiple semi-nested PCR reactions. The thermal profile of the PCR reactions was the following: 1 cycle of 95°C for 1 min, 39 cycles of denaturation at 95°C for 20 s, 50°C for 20 s, 72°C for 1.5 min, followed by an additional extension step for 10 min at 72°C . The PCR products were purified using a GeneJET PCR purification kit (Thermo-Fisher) according to the protocol provided by the manufacturer and sequenced directly using Big-Dye Terminator v1.1 Cycle Sequencing Kit (Thermo-Fisher) and run on an ABI 3500 Genetic Analyzer (Applied Biosystems, Hitachi, Tokyo, Japan). For sequence data analyses, the Chromas Ver. 2.6.6. and Geneious Prime ver. 2022.1.1 (Biomatters, New Zealand) software was used.

2.4. Bioinformatic analysis

Amino acid composition, estimated molecular weight, and theoretical isoelectric point analysis of *Ea*- β -catenin were executed by the ProtParam (ExpPASy) program. The secondary structure predictions were ascertained by the CFSSP program (ExpPASy). Following the BLAST analysis, *Ea*- β -catenin and β -catenin sequence homologues from various species were aligned by GeneDoc and UGene (Unipro, Russia) software [24]. Phylogenetic tree analysis was performed by MEGA 11 [25] with

the neighbour-joining method and 1000 bootstrap analysis was performed. The predicted protein model was built by SWISS-MODEL software and the conserved protein domain analysis was performed by SMART (EMBL, Germany).

2.5. Relative quantification of *Ea-β-catenin* mRNA

Various tissue samples of earthworms were collected from at least ten adult animals consecutively: pharynx, gizzard, midgut, ovarium, metanephridium, body wall, seminal vesicles, ventral nerve cord, and coelomocytes. A minimum of ten embryos were isolated in parallel from their cocoons, representing different developmental stages. Their precise progression state (from E1 to E4) was identified using well-defined morphological features by microscopic examination. For identification and major morphological features of embryonic stages (E1-E4) we refer to a scheme (Fig. S1) and its description in the Supplementary material [26,21]. For total RNA isolation from tissues and embryonic stages, we followed a similar procedure as we described earlier [21]. Following DNase I digestion (Amplification Grade DNase I, Sigma Aldrich), the reverse transcription was performed by High Capacity cDNA Reverse Transcription Kit (Thermo Fisher Scientific) using random hexamers according to the standard protocol. In each reaction, 1 µg DNase-treated total RNA was reverse transcribed and subsequently used as a template for PCR reactions. The final volume of reactions was 20 µL with resulting cDNA being stored at -20 °C until required. Synthesized cDNAs were directly used as a template for real-time quantitative PCR (qPCR) experiments. Gene-specific qPCR primers (Table S1) were designed with Primer Express software (Thermo Fisher Scientific) to evaluate the expression of the β-catenin gene in diverse tissues, as well as in embryo samples. Gene expressions were measured by an ABI Prism 7500 device (Applied Biosystems, Warrington, UK) using Maxima SYBR Green/Low Rox Master Mix (Thermo-Fisher). The amplification profile started at 95 °C and lasted for 10 min, followed by steps throughout 40 cycles: 35 s denaturation at 95 °C, 35 s annealing at 58 °C, and 1 min elongation at 72 °C. Dissociation curve analysis of amplified products was performed at the end of each reaction to confirm the generation of a single PCR product. *RPL17* mRNA level was implemented for normalization and gene expression level analysis was performed based on the $2^{-\Delta\Delta CT}$ method. The independent evaluations were repeated three times in duplicates.

2.6. Immunohistochemistry, immunofluorescence

Earthworm tissue segments (for explanation of major morphological characteristics of earthworm sections, please see the Supplementary material, Fig. S2) were placed into cryo-preservative embedding medium (Tissue-Tek O.C.T.) and sectioned at 8 µm with a Leica cryostat (Leica Biosystems, Deer Park, IL, USA) as previously reported [27]. After isolation, coelomocytes were spread onto glass slides by applying a Cytospin 3 centrifuge (SHANDON, Thermo Fisher Scientific). Firstly, after a 20-min fixation in 4 % ice-cold paraformaldehyde (PFA), slides were immersed in 0.1 % Triton X-100 (in PBS) for 20 min. For immunohistochemistry, endogenous peroxidase was inhibited by phenylhydrazine hydrochloride (Sigma, 1 mg/mL in PBS), in the case of immunofluorescence on coelomocytes; the autofluorescence was reduced by 0.1 M NH₄Cl solution. Before adding primary antibodies, non-specific binding was blocked with 5 % bovine serum albumin (BSA) for 20 min. For indirect labeling, a primary antibody (PY489-β-catenin monoclonal antibody, Developmental Studies Hybridoma Bank, Iowa City, Iowa; USA; 1:100 in 5 % BSA in PBS for 2 h at RT) and subsequently, HRP-conjugated anti-mouse immunoglobulins (rabbit polyclonal antibody, 1:100 in PBS for 1 h at RT, Dakopatts, Denmark) were applied to localize PY489-β-catenin in earthworm tissues. For immunofluorescence, Alexa-Fluor 647 conjugated goat anti-mouse IgM (µ chain) (Thermo Fisher Scientific, 1:500; 0.1 % in Triton-X/PBS) was employed as a secondary reagent for 1 h in the dark at RT. Subsequently,

cell nuclei were counterstained with DAPI solution (10 µg/mL, Sigma Aldrich) and slides were covered with a 1:1 mixture of PBS-glycerol. For immunohistochemistry, 3',3'-diaminobenzidine (Sigma) was used as chromogen in 0.1 M sodium acetate buffer (pH: 5.2), and Mayer's haematoxylin was employed for counterstaining. PY489-β-catenin monoclonal antibody (DSHB) recognizes a conserved epitope among various species [28] as demonstrated in Fig. S3. Control sections and cytoplasmic samples were incubated with non-immune mouse serum as primary reagent, then subsequently with HRP-conjugated anti-mouse immunoglobulin or Alexa-Fluor 647 conjugated goat anti-mouse IgM (µ chain). Images were taken using an Olympus BX61 microscope and AnalySIS software (Olympus Hungary, Budapest, Hungary).

2.7. *In vivo* and *in vitro* microbial stimuli

For the *in vivo* exposure, adult earthworms (three animals/condition) were treated with heat-inactivated *Escherichia coli* (ATCC 25922), *Staphylococcus aureus* (OKI 112001) (10⁸/mL each), zymosan (membrane from *Saccharomyces cerevisiae* in 1 mg/mL final concentration, Sigma Aldrich) and poly(I:C) (10 µg/mL, synthetic double-stranded ribonucleic acid, Miltenyi Biotec, Bergisch Gladbach, Germany) on filter paper for different time points (12 h, 24 h, 36 h, and 48 h, at RT) as previously described [21]. Briefly, the suspensions of microorganisms, zymosan, and poly(I:C) were diluted in LBSS, and control earthworms were exposed on *Lumbricus* Balanced Salt Solution (LBSS)-immersed filter paper (for detailed information on LBSS composition, please see the Supplementary Material). Three independent experiments were performed. After the treatments, coelomocytes were harvested [29] and their numbers were evaluated, then applied subsequently in gene or protein expression analysis.

For the *in vitro* treatments, the same conception was applied as we have previously described [29]. Following coelomocyte isolation, cell counting was performed. Coelomocytes (10⁶ cells in each condition) were incubated with heat-inactivated *E. coli* or *S. aureus* bacteria (10⁷), zymosan (0.2 mg/mL), or poly(I:C) (10 µg/mL) in 1 mL of RPMI-1640 medium supplemented with 10 % FBS and 1 % penicillin/streptomycin in 24-well plates (Falcon, BD Labware) for 3 h, 6 h, 12 h, and 24 h. Simultaneously at each time point, unexposed coelomocytes were used as controls. After incubations, cells were collected and washed two times in LBSS (100 RCF/5 min) and applied for gene or protein expression analysis (for technical details of SDS-PAGE and Western-blot analysis, please see the Supplementary material).

For the gene expression studies, total RNA extraction, reverse transcription, and qPCR experiments were performed as indicated above (Section 2.5), where *RPL17* mRNA level was employed for normalization. Normalized expressions of the *Ea-β-catenin* gene are exhibited in microbe-stimulated *E. andrei* earthworms compared to untreated ones.

2.8. Detection of cell proliferation and *Ea-β-catenin* expression during segment restoration

The design of earthworm regeneration experiments was based on the previously described protocols [27]. Briefly, earthworms were anesthetized in carbonated water (for 30–60 s) and then five anterior- and posterior-most segments were removed. During regeneration, earthworms were kept in soil at standard laboratory conditions [20]. One day before the removal of anterior or posterior regenerated segments, earthworms were placed on moist filter paper to empty their intestinal contents.

To detect cell proliferation during regeneration, we applied the Click-iT EdU Cell Proliferation Kit for Imaging with AlexaFluor 488 dye (Life Technologies, Carlsbad, CA, USA) following the same procedure as we have detailed earlier [27]. After EdU injections and anterior or posterior segment removal, tissues of the intact (control) and regenerating blastema (2 weeks/4 weeks) were stored in a Tissue-Tek O.C.T. cryo-preservative embedding medium at -80 °C. Sections for

simultaneous detection of proliferating cells and *Ea*- β -catenin were prepared based on a similar principle as before [27].

According to the manufacturer's protocol for EdU staining, sections were fixed in 4 % paraformaldehyde, and thereby, EdU slides were the subjects of immunofluorescence to detect *Ea*- β -catenin in earthworm tissues. For double labeling, slides were incubated in a blocking solution (3 % BSA in PBS for 30 min) before adding primary antibodies (PY489- β -catenin monoclonal antibody, DSHB, Iowa; 1:100 in 3 % BSA in PBS for 2 h in the dark at RT). After the incubation, slides were washed 3 times for 5 min with 0.1 % Triton-X/PBS. Alexa-Fluor 647 conjugated goat anti-mouse IgM (μ chain) (Thermo Fisher Scientific, 1:500; 0.1 % in Triton-X/PBS) was employed as a secondary reagent for 1 h in the dark at RT. Subsequently, cell nuclei were counterstained with Hoechst 33258 solution (10 μ g/mL, Sigma Aldrich) and sections were covered with a 1:1 mixture of PBS-glycerol.

Image acquisition and analysis were performed applying an Olympus ScanR (Olympus, Heidelberg, Germany) high-content screening station equipped with a multiband filter (M4DAFIC3C5, Chroma Technology GmbH, Olching, Germany), a highly sensitive digital CCD camera (C8484-05G02, Hamamatsu, Herrsching am Ammersee, Germany) and respective software, as instructed by the manufacturer. The center of each section was manually set using A1 centre calibration software. Based on the centre, an equal area was scanned on each specimen. We imaged 9×7 fields per section ensuring the complete scan of the designated area in every section, and to obtain reliable and comparable analysis and results. Following a manually set hardware autofocus, all coarse and fine focus processes were based on the mean intensity of Hoechst labelling (the first field was taken by all types of focuses, other fields only by the fine focus). Images were obtained with a $20\times$ objective (numerical aperture [NA], 0.45) in the fluorescence channels for blue (Hoechst), green (EdU), and red (β -catenin). Image processing was mainly based on Hoechst (to identify cells/nuclei as objects) and it began with background subtraction (to make a virtual channel) in all the images (all channels) to reduce noise. The segmentation algorithm was not applied. Watershed algorithm and ignoring of objects contacting with the field borders were also applied to separate individual cells from each other as much as possible and ensure that only whole cells were well detected. Co-localization of positive labelling in different channels (blue and green, blue and red, and blue and green and red) was detected, gated, and counted by the software. Fluorescent (e.g. mean and total intensity) and morphological parameters were also detected.

2.9. *In vitro* coelomocyte treatment by lithium chloride or iCRT14

Isolated coelomocytes (10^6 /ml) were cultured *in vitro* in a 24-well plate filled with RPMI cell culture medium supplemented with 10 % fetal bovine serum and a mixture of 1 % penicillin and streptomycin. Cultured coelomocytes were treated with lithium chloride (25 mM LiCl, Sigma-Aldrich) or iCRT14 (50 μ M, Sigma-Aldrich) for different time points. Control coelomocytes were cultured in the presence of appropriate concentrations of NaCl or DMSO, respectively. Following incubation periods, coelomocytes were centrifuged in LBSS, and then total RNA was isolated or cytopins were prepared from control and exposed coelomocytes for follow-up gene expression or immunofluorescence analysis, respectively.

2.10. Statistical analysis

Statistical analyses were carried out with GraphPad Prism 5.0 (GraphPad Software, Boston, MA, USA). The obtained data were checked for normality prior to further analysis (Shapiro-Wilk normality test). In the case of normal distribution, one-way ANOVA followed by Bonferroni multiple comparison *post hoc* test was applied to determine the significance of the data. If a non-normal distributed dataset was identified, a Kruskal-Wallis one-way analysis of variance followed by Dunn's multiple comparison test was executed. All data represent the

mean and standard error of the mean (\pm SEM) and $p < 0.05$ was marked as statistically significant.

3. Results

3.1. Identification and sequence analysis of *Eisenia andrei* β -catenin (*Ea*- β -catenin)

The full-length mRNA of *Ea*- β -catenin was obtained by overlapping several 5'- and 3'-RACE PCR results. The complete mRNA sequence is 3253 nt long, consisting of a 105 nt 5' untranslated region (UTR), a 649 nt 3'-UTR, and an open reading frame (ORF) of 2499 nt encoding a putative protein of 833 amino acid residues (Fig. 1). The estimated molecular weight of the protein is 90,860.49 Da, and the calculated isoelectric point (pI) is 5.96. The predicted protein does not possess a signal peptide or transmembrane domains. The *Ea*- β -catenin has a putative glycogen synthase kinase-3 (GSK-3) consensus recognition site of 23 amino acids located at the N-terminal region, followed by a 27 aa coiled-coil region, a central region of 11 armadillo/ β -catenin (ARM) repeats of 526 amino acids and a C-terminal region (Fig. 1).

3.2. Multiple sequence alignments, phylogenetic and structural analyses of *Ea*- β -catenin

Protein sequence homologue analysis (BLASTp) revealed that *Ea*- β -catenin protein (all query coverage above 97 %) evidenced the highest similarity to β -catenins isolated from Lophotrochozoan (annelids and mollusks) animal species. It showed 74.2 % identity with the β -catenin from polychaete annelid *Urechis caupo* (NCBI accession no. AAA30330), while it exhibited 72.9 % identity with another polychaete, the *Platynereis dumerilii* β -catenin (NCBI accession no. BQ85061). The β -catenin of brachiopod *Lingula anatina* (NCBI accession no. XP_013379954) has showed 73.98 % identity with the *Ea*- β -catenin protein. For other lophotrochozoans, certain mollusk species have a lower percentage of identity (71.03 % in the case of the oyster *Crassostrea gigas* (NCBI accession no. AFL93714), and 69.1 % with *Octopus sinensis* (NCBI accession no. XP_029634749)) with the earthworm *Ea*- β -catenin. While the arthropod *Panorpa germanica* (NCBI accession no. ROT66311) revealed 70.17 % identity, the chordate *Branchiostoma floridae* (NCBI accession no. AAY34439) revealed 70.71 %, and the human β -catenin (NCBI accession no. NP_001091679) displayed 67.88 % identities with *Ea*- β -catenin protein (Fig. 2). The multiple sequence alignment suggested four highly conserved phosphorylation sites (Ser46/50/59 and Thr54 in earthworm, corresponding to Ser35/39/47 and Thr43 in human, respectively) located in the GSK-3 consensus phosphorylation site. Thus, the hyperphosphorylated protein could be the subject of ubiquitin-dependent proteosomal degradation (Fig. 2).

A neighbour-joining (NJ) method of the phylogenetic tree (Fig. 3A) was constructed to visualize the relationship of *Ea*- β -catenin and its homologues from various invertebrate and vertebrate species. *Ea*- β -catenin, along with other annelids β -catenins such as from *Urechis caupo*, *Platynereis dumerilii*, *Chaetopterus varipedatus*, and *Capitella teleta* are clustered together (Fig. 3A). *Ea*- β -catenin exhibited a close evolutionary origin with other Lophotrochozoan (brachiopod and mollusk) β -catenin molecules. All the β -catenins from different animal groups are clustered into 11 major clades, such as the Cnidaria, Platyhelminthes, Nematoda, Mollusca, Annelida, Brachiopoda, Arthropoda, Hemichordata, Chordata, Echinodermata, Tunicata, and Vertebrate groups, correlating well with a putative topology of evolutionary origin. We observe that there is a high sequence relationship between the different species suggesting strong structural and functional conservation of β -catenin molecule. In the SWISS-MODEL prediction, we observed that the tertiary structure corresponds to the secondary structure (Fig. 3B) and we determined the GSK binding site location and the stable folded units of ARM domains each typically representing ~ 40 amino acids. The putative active sites Ser/Thr residues have been identified and

```

1  gtg tag tct gtg ttt tgt acc ttt gtg gtt gga att ttt cgt ctt cgt aat ttc ttc gta
61  atc ttc gta att ttg cac tca att ttg ctg gat tga gca gtg gct ATG TCC GTG TAC CAA
                                M S V Y Q
121 CAG TCG GGAATG GCT TCC CGT CAA GGT CCA GGT CAG CAC TAC ATG GAC CTT GGA TCAATG
    Q S G M A S R Q G P G Q H Y M D L G S M
181 GAC AAC AAG CAG CAC CAG ACA TTG ATG TGG CAG CAG GGG CAG TAT ATG TCT GAT TCA GGC
    D N K Q H Q T L M W Q Q G Q Y M S D S G
241 ATC CAC TCC GGA CTG ACC ACT CAC GGT CCT CCT TCG GTC AGT AGC AAG CAC GGC CTG GAT
    I H S G L T T H G P P S V S S K H G L D
301 GAA ATG GAG ACC GGA AAT GAG ATG GAC ACT ACG CAG ATG ATG TTT GAT TTT GAC CAG GGA
    E M E T G N E M D T T Q M M F D F D Q G
361 TTC AAC CAA GGG TTC ACC CAG GAA CAA GTC GAT GAG ATG AAC CAG CAG TTG AAT CAA ACT
    F N Q G F T Q E Q V D E M N Q Q L N Q T
421 CGT TCG CAG CGT GTG CGT GCC GCAATG TTC CCA GAG ACC CTT GAG GAA GGG TTC CAG ATT
    R S Q R V R A A M F P E T L E E G F Q I
481 CCC TCG ACC CAG ATC CAC CCG GGT CAG TCG ACT GCA GTT CAG CGC CTC GCT GAA CCA TCT
    P S T Q I H P G Q S T A V Q R L A E P S
541 CAG ATG CTG AAG CAT GCT GTT GTC AAC CTC ATC AAC TAC CAG GAT GAT GCT GAT TTG GCG
    Q M L K H A V V N L I N Y Q D D A D L A
601 ACT AAG GCA ATT CCT GAA TTG GCG AAG CTG TTA ACG GAT GAG GAC CAA GTG GTT GTT GGT
    T K A I P E L A K L L T D E D Q V V V G
661 CAG GCG GTC ATG ATG GTC CAT CAA CTG TCA AAG AAG GAA GCC AGT CGC CAT GCC CTC ATG
    Q A V M M V H Q L S K K E A S R H A L M
721 AAC TCC CCC CAG ATG ATT GCT GCC CTC ATT CGG GCT ATG TCG ACT ACC TCT GAC CCG GAG
    N S P Q M I A A L I R A M S T T S D P E
781 ACA ACT CGA TGC ACA GCT GGA ACT CTG CAT AAC CTT TCT CAC CAT CGC CAA GGA CTG CTT
    T T R C T A G T L H N L S H H R Q G L L
841 GCT ATA TTT AGA TCG GGT GGA ATT CCC GCT CTT GTC AAG CTC CTG AGT TCT CCG ATT GAG
    A I F R S G G I P A L V K L L S S P I E
901 TCT GTC TTG TTC TAC GCG ATT ACA ACA CTT CAC AAT CTG CTG CTG CAC CAG GAA GGT GCC
    S V L F Y A I T T L H N L L L H Q E G A
961 AAG ATG GCA GTC CAT CTT GCT GGA GGG TTG CAG AAG ATG GTT GCC CTA TTG CCC AGA AAC
    K M A V H L A G G L Q K M V A L L P R N
1021 AAT GTC AAG TTC CTT GCC ATA ACA ACT GAC TGT CTC CAG ATT TTG GCT TAT GGC AAC CAA
    N V K F L A I T T D C L Q I L A Y G N Q
1081 GAG AGC AAG TTG ATC ATC CTG GCA AGT GGA GGT CCA GCA GAG TTG GTC CGC ATC ATG GCT
    E S K L I I L A S G G P A E L V R I M A
1141 ACA TAC ACG TAT GAG AAG TTG CTT TGG ACA ACC TCA AGG GTT CTG AAG GTT CTT TCG GTC
    T Y T Y E K L L W T T S R V L K V L S V
1201 TGC CCC AGC AAC AAA GCC GCA ATT GTT GAA GCA GGT GGC ATG GGT GCA ATG GCA ATC CAT
    C P S N K A A I V E A G G M G A M A I H
1261 CTC AAT CAT CAG AGT CAG CGA CTG GTA CAG AAT TGC CTC TGG ACG CTT CGT AAT CTC TCT
    L N H Q S Q R L V Q N C L W T L R N L S
1321 GAT GCT GCT ACC AAA GTG GAT GCG ATG GAC ACT CTT CTC CAG ACC CTG GTT TCG CTT CTC
    D A A T K V D A M D T L L Q T L V S L L
1381 ACT TCC AGT GAC ATA AAC ATT GTG ACC TGT ACG GCT GGA ATC CTT TCC AAC CTG ACC TGT
    T S S D I N I V T C T A G I L S N L T C
1441 AAC AAC CAT CGT AAC AAA GTG GTT GTC TGC CAG GTC GGA GGA ATT GAG GCT CTC GTT CGA
    N N H R N K V V V C Q V G G I E A L V R
1501 ACC ATC ATC CAG GCT GGA GAG AGG GAT GAC ATC ACA GAA CCA GCA GTG TGT GCC CTG CGT
    T I I Q A G E R D D I T E P A V C A L R
1561 CAT CTG ACC AAT CGT CAT TCA GAG GCG GAG ATG GCC CAG AAT GCA GTT CGG CTG CAT TAC
    H L T N R H S E A E M A Q N A V R L H Y
1621 GGA CTG CCA GCA ATC GTAAAG CTC CTT CAT CCT CCG AGT CGT TGG CCT TTG ATC AAG GCC
    G L P A I V K L L H P P S R W P L I K A
1681 GTC ATC GGC CTC ATC CGC AAT CTC GCG CTC TGC CCT GCG AAC AAT GCG CCA TTG AGG GAA
    V I G L I R N L A L C P A N N A P L R E
1741 CAT GGA GCG ATT CCA CGT TTA GTC CAG CTT CTG ATT CGT GCT CAT CAG GAC ACA CAA AGG
    H G A I P R L V Q L L I R A H Q D T Q R

```

Fig. 1. Sequence analyses of *Ea-β-catenin*. Full-length nucleotide and deduced amino acid sequence of *Ea-β-catenin*. The start codon is in bold, and the stop codon is indicated by an asterisk. The complete length of *Ea-β-catenin* is 3253 nt, including an open reading frame (ORF) of 2499 nt, encoding a putative protein with 833 amino acid residues that consists of 11 armadillo (ARM) repeat regions. The ORF of the nucleotide sequence is shown in upper case letters, while the 5' and 3'UTR sequences are in lower case. The putative GSK-3 consensus phosphorylation site is boxed, while the armadillo repeat regions are shaded with grey. The coiled-coil region is underlined, and the amino acid sequence regulating gene transcription is double-underlined.

highlighted on the tertiary structure of the *Ea-β-catenin* (Fig. S4).

The protein sequence and SMART analysis of *Ea-β-catenin* predicted the presence of 11 ARM repeats spanning amino acid residues of

157–196, 197–239, 240–280, 281–322, 324–365, 366–406, 446–489, 494–535, 536–601, 602–642, and 643–683. Between ARM6 and ARM7, a low complexity region of 12 amino acids is located (Figs. 1 and 3C).

```

1801 CGT CCT GGA CCA GGG GCA GCAAAC CCA GGC CAG GGAACA TTT GTC GAT GGT GTG AGG ATG
    R P G P G A A N P G Q G T F V D G V R M
1861 GAG GAG ATT GTG GAG GGT ACA GTT GGC GCT CTG CAC ATC TTG GCA CGC GAG AGT CAT AAC
    E E I V E G T V G A L H I L A R E S H N
1921 AGG GCT GTT ATC CGC ACC CTC AAC TGC ATC CCA CTG TTC GTT CAG TTG CTG TAT TCT CCA
    R A V I R T L N C I P L F V Q L L Y S P
1981 ATT GAG AAT ATC CAG CGT GTC GCA GCC GGT GTC CTT TGT GAA CTG GCG GCC GAG AAG GAA
    I E N I Q R V A A G V L C E L A A E K E
2041 GGG TCA GAG GCC ATC GAA CAA GAG GGC GCC ACT GCA CCT CTC ACG GAA CTA CTG CAC AGT
    G S E A I E Q E G A T A P L T E L L H S
2101 CGC AAT GAA GCT GTC GCG ACC TAT GCA GCT GCT GTT CTG TTC CGT ATG AGC GAT GAC AAA
    R N E A V A T Y A A A V L F R M S D D K
2161 TCA CAG GAC TAC AAG AAG CGA CTG TCG GTT GAG CTG ACA AGC TCT CTC TTC CGT GGC GAC
    S Q D Y K K R L S V E L T S S L F R G D
2221 CCA GCT GAT TGG AAT GAG CCC CCA ATG CTT GAT GAG GCA ATG AAC GAT GAG ATG TAT CGC
    P A D W N E P P M L D E A M N D E M Y R
2281 AGG AAT CAA CCA ATG GTT GAA ACC GGT TAC AAC CAG ATG GCC CAC CAG GGA ATG GGT CGA
    R N Q P M V E T G Y N Q M A H Q G M G R
2341 GAC ACA GAT TAT GAC CCA GTG GGG TCA ATG CAG GGT TAT GTC ATC GGT CAC CAA GGC TAT
    Q T D Y D P V G S M Q G L V I G H Q G Y
2401 GGT CCC GGC AGC ATT TCA GAT GTG GGT GCT TAT CCC CAG GGT CCC CAT CCA GGA GCC ACT
    G P G S I S D V G A Y P Q G P H P G A T
2461 CAT CTT CCC GAC CTG GGG CAG GGA ATG TCG CCC CAC TAT GAT GGC TCT GAC GTT TCG AGC
    H L P D L G Q G M S P H Y D G S D V S S
2521 ACC ACC GGT CAT CAG ATG CAC ATC GGG GGT GCA CTG AAC CCC TCT GAC CCATCA CAG ATG
    T T G H Q M H I G G A L N P S D P S Q M
2581 GGT GCC TGG TTC GAC AGT GAT GTG TAA gca tgg aga cct tgg tca tcc tgg agc att acc
    G A W F D S D V *
2641 atg gaa atc ctg gtt gtc agt ggt gat cgg cca tgc gtt acg atg taa tct cga ctt tag

2701 atg ttc tgt gag act ttt aga tgt tct gtg aga cta att tta taa tct cta aga acg gtc

2761 gtt gcc ctt ggt gat tta ttc att acc ttt ggt gat aaa ttc gtt gcc ctt ggt gat tta

2821 ttc gtt gcc ttt ggt gat gaa ttc gtt gcc ctt ggc gat tta ttc gtt gcc ttt ggc gat

2881 aga ttc gtt gcc ctt ggt aat tta ttc gtt gcc ttt ggt gat gaa ttc gtt gcc ctt ggt

2941 gat tta ttc gtt gcc ttt ggt gat aga ttt gtt gcc tgc tgc tct gaa tga cga att ctc

3001 tgc cct tgg caa tgg atg gtt ggt cag att cat gag caa gtc aat ggt tcc gag att tgt

3061 gac aaa gct tga cag ggt gta ggg agg gtc aaa ttg gtc aaa aat aac atg acg tac ttt

3121 att gat ggc acc taa tat tat taa gat taa tag atg acg att atg tct gta taa tat gtg

3181 aat ggt taa cag ttt gtg cta aac gtg gta act gtt ttg aat aga tac att gaa tgg taa

3241 aaa aaa aaa aaa a

```

Fig. 1. (continued).

3.3. Embryonic expression pattern and adult tissue distribution of *Ea-β-catenin*

Earthworm ontogenesis begins in cocoons and can be subdivided morphologically into four major embryonic stages (E1-E4, respectively) [26]. Gene expression (qPCR) analysis revealed that *Ea-β-catenin* mRNA is present during all four stages of earthworm embryonic development (Fig. 4A). Furthermore, its expression has evidenced a gradual increase over time from E1 to E4 stages, and E4 stage (before hatching) has significantly higher *Ea-β-catenin* mRNA message compared to the E1 and E2 stages (Fig. 4A).

Subsequently, total RNA samples were isolated from several different tissues of adult earthworms to compare their *Ea-β-catenin* mRNA levels (Fig. 4B). Our results indicated the ubiquitous, but variable expressions of *Ea-β-catenin* in the following tissues: low levels in pharynx, intestine, and seminal vesicles, moderate levels in body wall, gizzard, and coelomocytes, high levels in ovary, metanephridium and the ventral nerve cord. Using immunohistochemistry, we observed a weak signal in the gut (Fig. 4C) with the PY489-β-catenin-specific mAb, which recognizes a

conserved epitope illustrated in Fig. S3. Moderate signals were detected in the body wall and coelomocytes located in the coelomic cavity (Fig. S5A, B) compared to the appropriate negative control (Fig. S5C, D). Coelomocytes are mesoderm-derived circulating innate immune cells of the earthworms. Two major subpopulations (amoebocytes and eleocytes) have been characterized by morphological and functional methods. Amoebocytes are responsible for effector immune functions (eg. phagocytosis), while eleocytes secrete antimicrobial and nutritive factors [29,30]. To determine the *Ea-β-catenin* mRNA expression in the different coelomocyte subpopulations, we separated the coelomocyte subsets (amoebocytes vs. eleocytes) by cell sorting (as we described earlier) [29,30] and subsequently isolated total RNA from them. Among the sorted amoebocytes and eleocytes, only the amoebocyte subpopulation expressed the *Ea-β-catenin* mRNA (Fig. S5E). Immunocytochemical staining provided proof for this previous observation, since amoebocytes have shown a positive cytoplasmic signal, while a cluster of small, aggregated cells exhibited nuclear localization of PY489-β-catenin compared to the consistently unstained eleocytes (Fig. 4D).

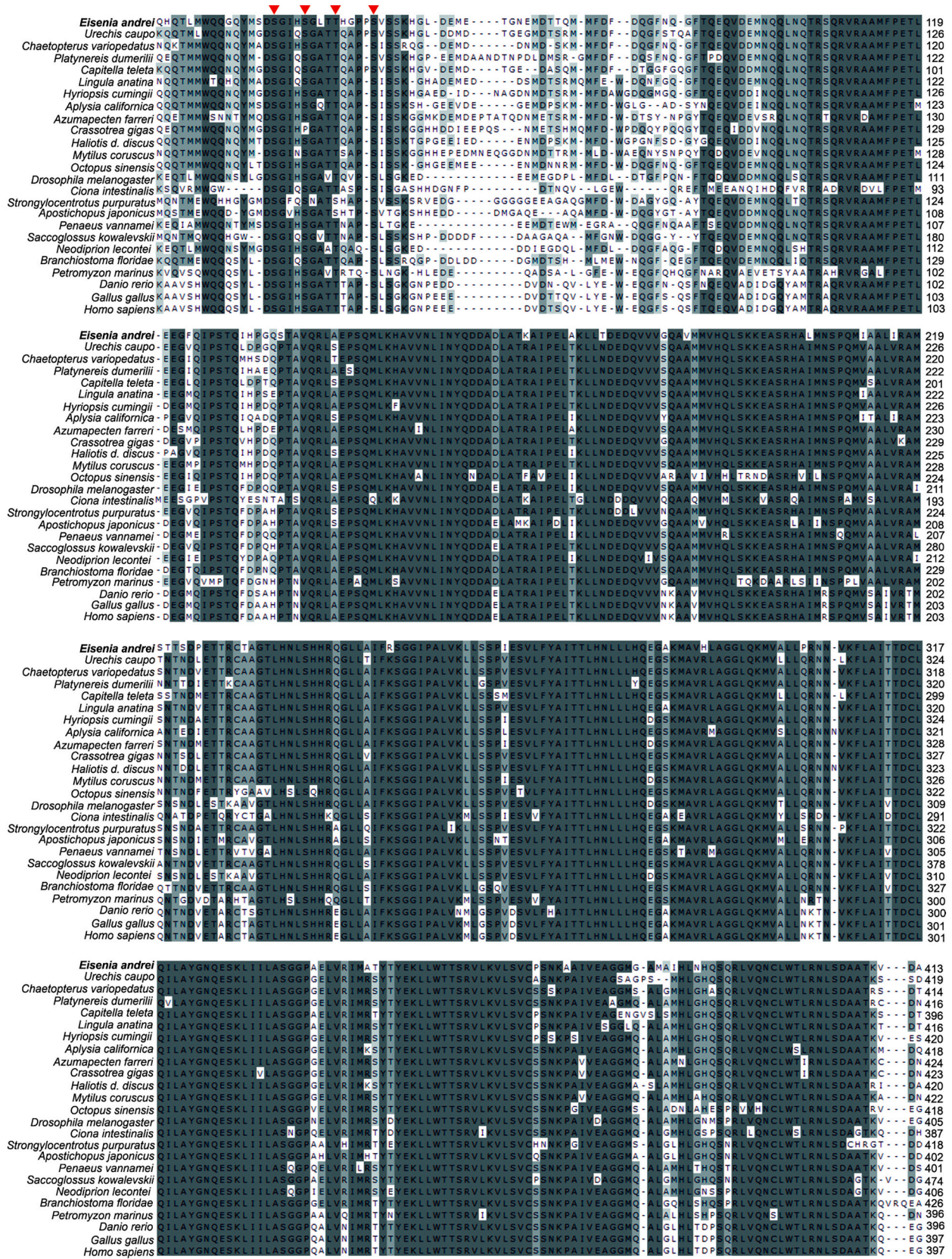


Fig. 2. Multiple sequence alignment of β-catenin proteins from different invertebrates (*E. andrei* is marked in bold letters) and vertebrate species. The identical residues are shaded by dark grey and light/pale grey color indicates highly conserved or semi-conserved amino-acid substitutions. The conserved phosphorylation sites are indicated with a red triangle.

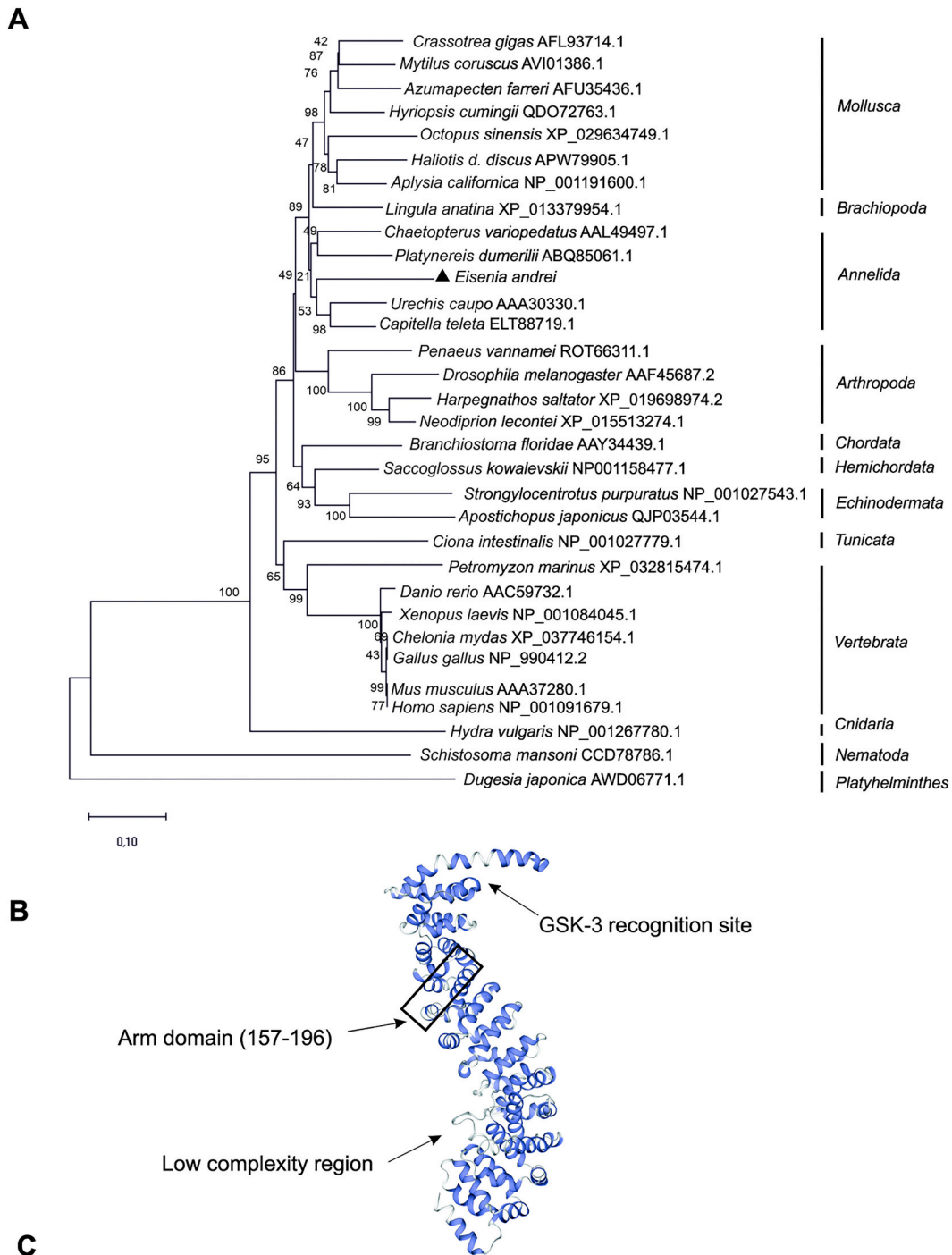


Fig. 3. The phylogenetic tree of β -catenins from different organisms (A). Phylogenetic relationship analysis based on the deduced amino acid sequences of *E. andrei* β -catenin (marked with a black triangle) with the closest annelid species and other related molecular relatives by the maximum likelihood method conducted by MEGA11. The numbers close to the branch nodes represent the percentage of 1000 bootstrap replications. The tree is drawn to scale, with branch lengths in the same units as those of the evolutionary distances used to infer the phylogenetic tree. Accession numbers are provided following the species name (A). Predicted 3D structural model of *Ea*- β -catenin highlighting the GSK-3 binding site, the first Armadillo domain, and the low complexity region (B). SMART-based architecture and location illustration of conserved domains (including the characteristic 11 ARM domains) of *Ea*- β -catenin (C).

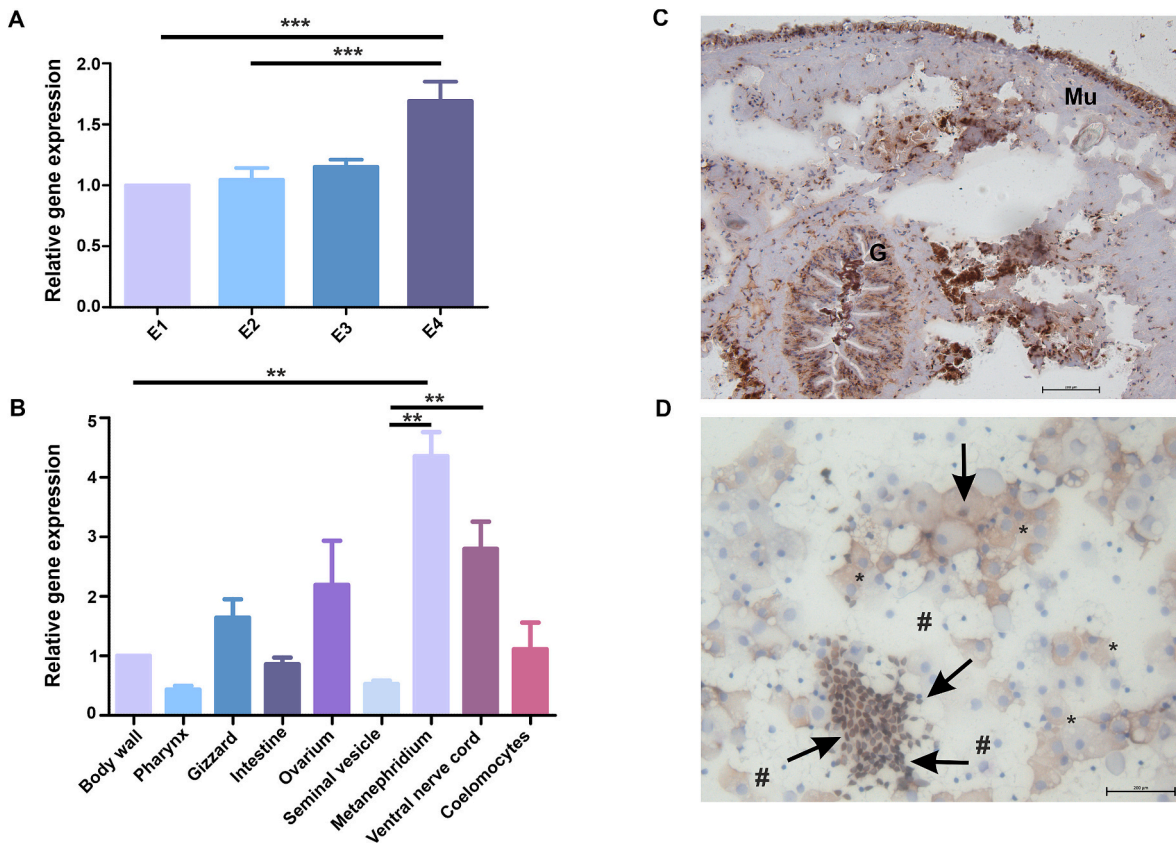


Fig. 4. Differential expression levels of *Ea-β-catenin* mRNA during earthworm ontogenesis. E1-E4 denote morphologically different embryonic stages (A). Tissue distribution of *Ea-β-catenin* in adult earthworms measured by quantitative PCR (B). Quantitative measurements were normalized to *E. andrei RPL17* mRNA levels. Relative expression values are given as mean \pm SEM ($n = 6$). Asterisks indicate significant differences ($p^{**} < 0.01$, $p^{***} < 0.001$, Kruskal-Wallis). Immunohistochemistry of adult *E. andrei* earthworm cross-section applying the PY489- β -catenin specific monoclonal antibody. Mu - muscle layers, G - gut. Scale bar: 200 μ m. (C). Immunocytochemistry of PY489- β -catenin monoclonal antibody labeled coelomocytes. Number signs (#) denote cytoplasmic signal of PY489- β -catenin mainly in amoebocytes, while nuclear translocation of PY489- β -catenin (arrows) can be observed in a cluster of cells. Eleocytes appear consistently negative (asterisks). Scale bar: 200 μ m (D).

3.4. Postembryonic expression of *Ea-β-catenin* and cell proliferation kinetics during anterior and posterior regeneration

Earthworm segment regeneration was initiated by the removal of the last 5 segments at the anterior or posterior ends (for explanation of earthworm segment regeneration please see the scheme in the Supplementary material, Fig. S6). Injury-induced cell proliferation was observed upon EdU reagent injection into the anterior or posterior segments of regenerating earthworms along with intact animals (Figs. 5A-C, 6A-C, S7A, B). Similarly to our previous observation [27], we found the highest amount of EdU⁺ cells (with intense proliferation rate) in the 2nd week (Figs. 5B, D and 6B, D), while the proliferation rate was attenuated in 4th week (Figs. 5C, D and 6C, D) during both anterior and posterior restoration periods. For EdU⁺/PY489- β -catenin⁺ cells, we observed a significant increase during the 2nd and 4th posterior regeneration compared to the intact segments (Fig. 6D). In addition, the number of single PY489- β -catenin⁺ cells evidenced a slight increase during the 2nd week of anterior regeneration (Fig. 5D), while it dropped significantly during 2nd and 4th weeks of posterior tissue restoration (Fig. 6D) compared to the intact segments. Higher magnifications of immunofluorescence analysis (Figs. S7A, B and S8A) reveal nuclear translocation of PY489- β -catenin (please see Fig. S8B as the negative control of tissue immunofluorescence).

Besides the cellular expression of β -catenin in regenerating earthworms, we monitored the *Ea-β-catenin* mRNA levels in the restored segments at similar time points. First, we observed a slight, significant decrease in *Ea-β-catenin* mRNA in the 2nd week of anterior regeneration,

then it significantly increased in the 4th week of regeneration (Fig. 5E). In the case of posterior segment restoration (Fig. 6E), *Ea-β-catenin* mRNA expression showed a different pattern, peaking in the 1st week, then significantly dropping in the 2nd week, and slowly increasing by the 4th week of regeneration.

3.5. *Ea-β-catenin* expression levels upon different microbial challenges

To test the involvement of *Ea-β-catenin* in the innate immune response of *E. andrei* earthworms, we exposed *in vitro* cultured coelomocytes and earthworms *in vivo* to various microbes or microbial compounds. Then, we measured the *Ea-β-catenin* mRNA and *Ea-β-catenin* protein levels from the *in vitro* or *in vivo*-exposed coelomocytes to the Gram-negative *E. coli* and Gram-positive *S. aureus* bacteria strains, zymosan of *S. cerevisiae*, and the synthetic dsRNA, poly(I:C) (Fig. 7). Short-term (3–6 h) *in vitro* stimuli of *S. aureus* bacteria strains caused a non-significant increase in *Ea-β-catenin* mRNA level, while at 6 h and 12 h Poly(I:C) and zymosan induced a significant elevation in mRNA level. At a later time point (24 h), *E. coli* caused a significant increase in the *Ea-β-catenin* mRNA expression, in contrast to an earlier time point (6 h) and to the non-significant fluctuation with *S. aureus* treatment (Fig. 7A). Western blot analysis revealed a non-significant decrease of PY489- β -catenin protein levels upon the *in vitro* 6 h Poly(I:C) treatment (Fig. 7B) when compared with control coelomocytes (Fig. 7C). Early time points (12 h) of *in vivo* poly(I:C) treatment caused a transient, non-significant increase of *Ea-β-catenin* mRNA, but it was significantly attenuated at 24 h (Fig. 7D). A later time point (48 h) of *in vivo* treatments with *E. coli*

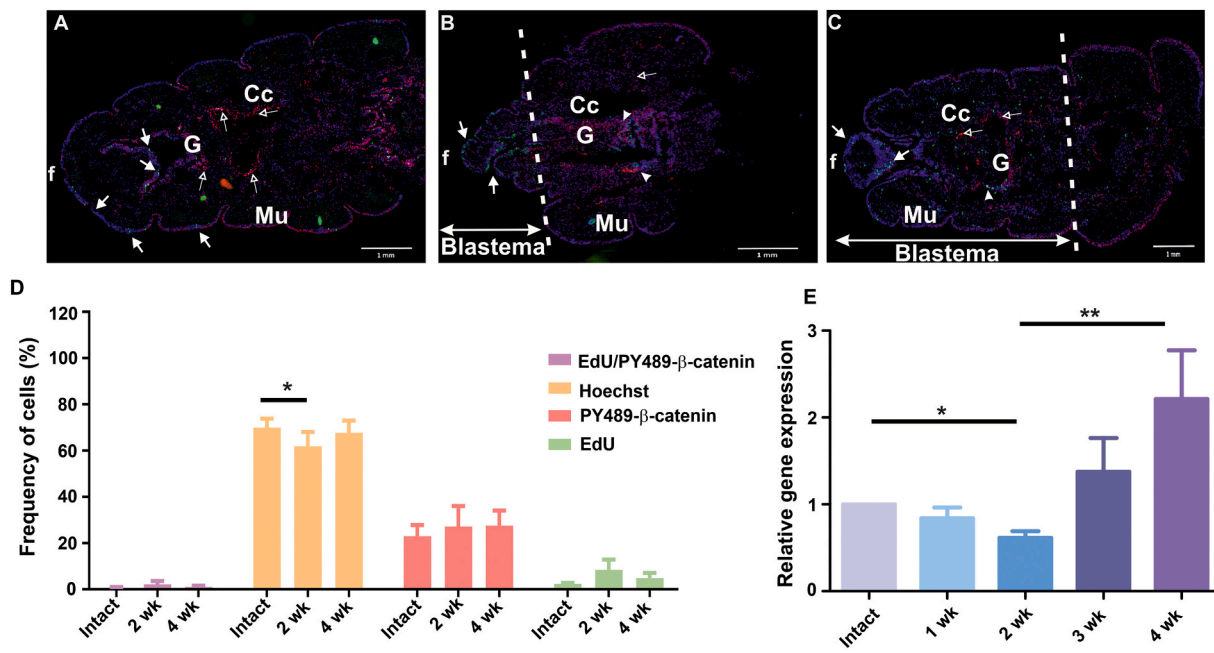


Fig. 5. Immunofluorescence analysis of PY489-β-catenin expression (red color, white, outlined arrows) along with EdU-incorporation-based cell proliferation (green color, solid white arrows) in the tissues of intact (A), 2-week (B), and 4-week (C) anterior regeneration of *E. andrei* earthworms (merged images are shown). Nuclear counterstaining was performed with Hoechst dye (blue color). The blastema of regenerating tissue is marked by a dashed line. EdU⁺/PY489-β-catenin⁺ cells are highlighted with white arrowheads. Representative images were chosen from eight independent experiments. Cc – coelomic cavity, f - anterior or front end, G - gut, Mu - muscle layers. Scale bar: 1 mm (A-C). Bar chart represents the frequencies (%) of EdU⁺/PY489-β-catenin⁺ cells, Hoechst-, PY489-β-catenin-, and EdU-positive cells in intact, 2- and 4-week-old restored blastema during anterior earthworm regeneration (D). Expression levels of *Ea-β-catenin* mRNA during the anterior regeneration from 1 to 4 weeks (E). Relative gene expression pattern in the regenerating blastema was compared to intact segments and expression values represent the mean ± SEM (n = 6). Asterisks denote significant differences (*p < 0.05, **p < 0.01; Kruskal-Wallis) (D, E).

bacteria strain induced a significant elevation, while 36 h Poly(I:C) treatment evoked only a transient, yet significant increase in *Ea-β-catenin* mRNA level (Fig. 7D). PY489-β-catenin level increased only transiently at 36 h following the *in vivo* *E. coli* exposure (Fig. 7E, F).

3.6. Activation or inhibition of *Ea-β-catenin* following *in vitro* exposure by bioactive small molecules

Coelomocytes were exposed *in vitro* to 25 mM LiCl or 50 μM iCRT14 (with appropriate amounts of NaCl or DMSO for negative controls, respectively) at different time points. Subsequently, total RNA was isolated, and then we monitored the *Ea-β-catenin* mRNA expression. At a later time point (24 h), LiCl treatment significantly increased *Ea-β-catenin* mRNA levels compared to earlier time points and control samples (Fig. 8A). In a follow-up experiment, immunofluorescence analysis of PY489-β-catenin was performed on NaCl- and LiCl-exposed coelomocytes (Fig. 8B, C). We clearly demonstrated the nuclear translocation of PY489-β-catenin in LiCl-exposed coelomocytes (Fig. 8C) compared to NaCl-treated coelomocytes (Fig. 8B).

In contrast, the Wnt/β-catenin pathway inhibitor iCRT14 had an opposing effect, once we found a significant decrease of *Ea-β-catenin* mRNA expression already at early time points of the experimental design (Fig. 8D). Immunofluorescence analysis of iCRT14-exposed coelomocytes revealed an opposing effect, while we detected certain nuclear signals of PY489-β-catenin in DMSO-treated coelomocytes (Fig. 8E) that decreased in the iCRT14-incubated coelomocytes (Fig. 8F) (please see Fig. S8C as the negative control of cytospin immunofluorescence).

4. Discussion

Wnt/β-catenin pathway controls cell fate through an array of mechanisms with the β-catenin representing a key molecular

component. This pathway plays a critical function in animal body plan morphogenesis due to its pivotal role in intracellular signaling and cell adhesion [2]. This molecule is evolutionarily well-conserved from invertebrates to chordates; however, we know relatively little about its expression and role in terrestrial annelids.

In this study, for the first time, we identified and characterized a β-catenin homologue from the earthworm *E. andrei*. Sequence analysis showed that *Ea-β-catenin* has a conserved primary structure that is highly similar to other β-catenin molecules. In general, it contains an N-terminal structure, a central region with 11 ARM repeat domains, and a C-terminal region (Figs. 1, 3B, and C). At the N-terminal end, four conserved amino acids can be found as Ser46, Ser50, Ser59, and Thr54 in the consensus GSK-3 binding site (Figs. 1 and 2) that could be phosphorylated by GSK-3, and subsequently, the hyperphosphorylated β-catenin can be a target for the ubiquitin-proteasome complex-mediated degradation [17,31]. In addition, the classical, continuous ARM-repeat domains of β-catenin are composed of ~40 AAs sharing similar tandem copies of sequence motifs to form a highly conserved three-dimensional structure. The ARM-repeat domains of *Ea-β-catenin* show 84 % of identity with a β-catenin from the chordate *Branchiostoma floridae*. It was proven in mammals that the ARM repeats of β-catenin are engaged with several molecular ligands. They exert various functions, such as controlling cell signaling by the transcription factor TCF/LEF-1 or facilitating its own degradation by Axin, APC, and GSK-3 [5]. It is suggested that the β-catenin molecule is less conserved at the C-terminal end [17] compared to N-terminus and ARM repeats. Indeed, a type I PDZ binding motif (D-T-D-L) can be found at the C-terminal end of several typical β-catenins [32]; however, the C-terminal domain of *Ea-β-catenin* contains a slightly different motif (D-S-D-V) (Fig. 1), whether this change influences its molecular functions requires further investigation. Moreover, the phylogenetic analysis suggested that *Ea-β-catenin* shares strong homology (above 71 %) with other Lophotrochozoan (especially annelid) β-catenins (Figs. 2 and 3A). These results obtained from

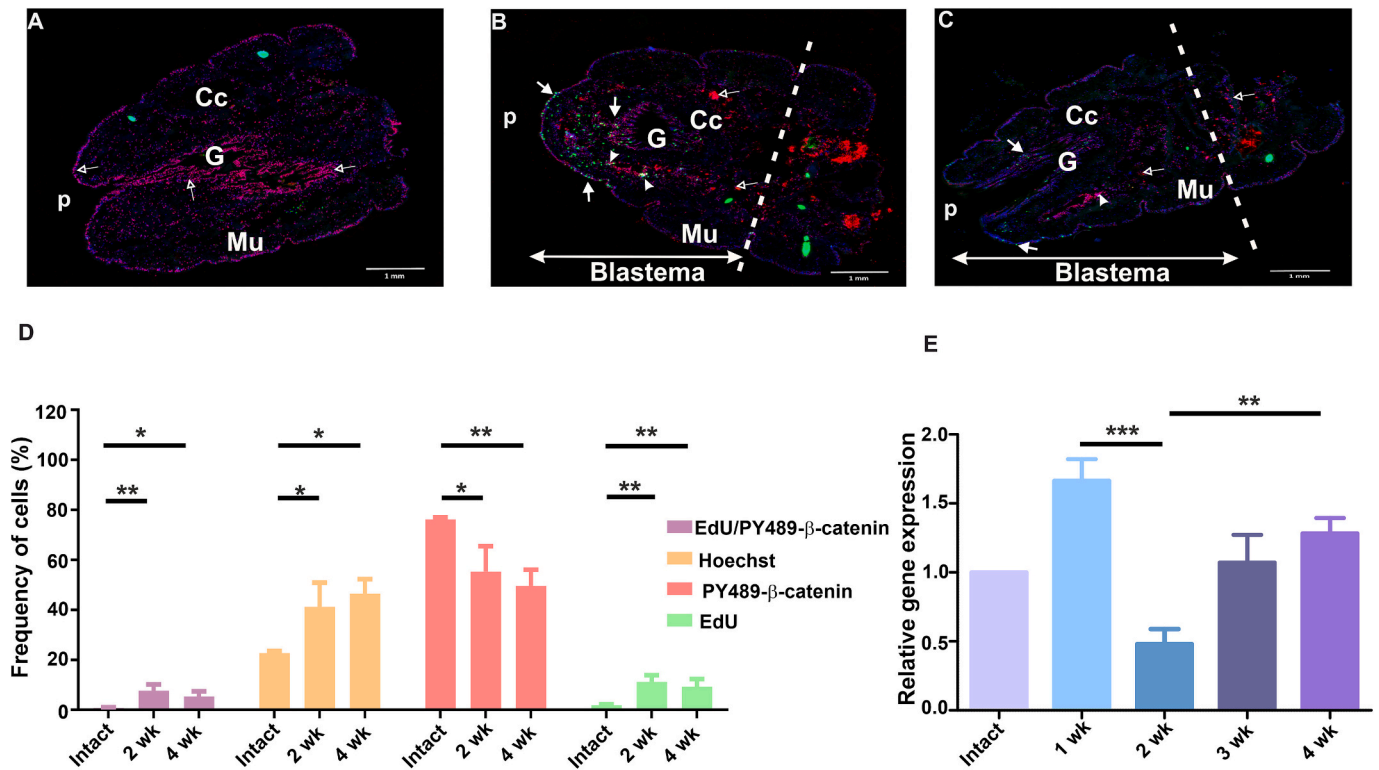


Fig. 6. Immunofluorescence detection of PY489-β-catenin (red color, white outlined arrows) and evaluation of EdU-incorporation-based cell proliferation (green color, solid white arrows) kinetics in intact (A), 2- (B) and 4-week-old (C) blastema of *E. andrei* earthworms during posterior segment regeneration (merged images are shown). Nuclear counterstaining was performed by Hoechst dye (blue color). EdU⁺/PY489-β-catenin⁺ cells are highlighted with white arrowheads. Dashed lines denote the blastema in 2- and 4-week-old regenerating animals. Eight independent experiments were performed, and representative pictures are shown. Cc – coelomic cavity, G - gut, Mu - muscle layers, p – posterior end. Scale bar: 1 mm (A-C). Bar chart corresponds to the frequencies (%) of EdU⁺/PY489-β-catenin⁺ cells, Hoechst-, PY489-β-catenin-, and EdU-positive cells in intact, 2- and 4-week-old earthworms during posterior regeneration (D). Expression pattern of *Ea-β-catenin* mRNA levels from 1 to 4 weeks of posterior regeneration (E). Relative gene expression pattern in the regenerating blastema was compared to intact segments and expression values show the mean ± SEM ($n = 8$). Asterisks indicate significant differences (* $p < 0.05$, ** $p < 0.01$, *** $p < 0.001$; Kruskal-Wallis) (D, E).

sequence and structural analysis suggest that *Ea-β-catenin* has very similar functions to its invertebrate and vertebrate homologues. Indeed, β-catenin belongs to the extensive catenin protein family consisting of α-catenins, β-catenins and δ-catenins subfamilies. So far, one characteristic member of each subfamily has been identified in Lophotrochozoans [3]; however, we cannot rule out the possibility that orthologues can be found later in this animal group.

The Wnt/β-catenin pathway is crucially important in embryogenesis and tissue morphogenesis of vertebrates [33]. Now, it is generally accepted that this morphogen pathway also controls the larval morphogenesis and gametogenesis in various invertebrates [17,34]. In annelids, β-catenin is involved in the cell fate specification during the larval development of the polychaeta *Platynereis dumerilii* [35] and in the larval metamorphosis of *Pseudopolydora vexillosa* [36]. During *E. andrei* embryogenesis, we observed the presence of β-catenin mRNA in all four embryonic stages, and it gradually increased at the E4 stage (Fig. 4A), underscoring the importance of β-catenin in earthworm ontogenesis. The comprehensive tissue distribution of β-catenin has been reported from several invertebrate species [12,13,37,38]. Similarly, *Ea-β-catenin* mRNA and protein were expressed in all tested tissues but at different levels in adult earthworms (Fig. 4B, C). Interestingly, ovarium, metanephridium, and ventral nerve cord have the highest level of expression, while coelomocytes, body wall, and intestine have moderate levels (Fig. 4B). It is well reported that β-catenin has an inevitable role in mammalian female gonad development [39]; however, we know very little about the molecular control of sex determination and gonad development in Lophotrochozoan invertebrates [40]. According to Santerre et al. [41], β-catenin is engaged in ovarium development of the mollusk *Crassostrea gigas*. Indeed, our data also suggests that in *E. andrei*

earthworms, *Ea-β-catenin* is a characteristic component of female gonad structures (ovary) compared to male ones (seminal vesicles) (Fig. 4B). In this regard, β-catenin is strongly involved in ovary development of invertebrates, similarly to mammalian female gonad development [39]. During mammalian kidney development, three kidney structures can be observed: the transient pronephros and mesonephros, versus the permanent kidney-forming, metanephros. During embryogenesis, the Wnt/β-catenin pathway is involved in all three kidney types [2,42,43], however, it has a more extensive role during nephron formation (a mesenchymal to epithelial transition of metanephros) [44] due to Wnt4 signaling. The presence of beta-catenin in invertebrate kidneys is less explored, however, its expression has been reported in *Hyriopsis cumingii* mussels [13], and our data also supports its importance in invertebrate (earthworm nephridia) kidney homeostasis.

During a post-embryonic developmental process (e.g. regeneration), β-catenin expression is critical for normal tissue restoration as reported from numerous (invertebrate or vertebrate) animal models [45–48]. A recent transcriptomic study indicated its involvement in axial (segment) regeneration of the freshwater Oligochaeta annelid *Pristina leidyi* [18].

Earthworms possess high regeneration capacity involving the complete restoration of several segments at the injured anterior or posterior sites. This process is well-documented morphologically, though its molecular mechanisms are still obscured [27], but now novel data is emerging [49]. The underlying tissue restoration machinery involves both reorganization of old segments (e.g. morphallaxis) and formation of a blastema (a cluster of undifferentiated, progenitor cells) during epimorphosis process [27].

In regenerating *E. andrei* earthworms, the EdU-labeling-based cell tracing analysis revealed increased cell proliferation by the 2nd week of

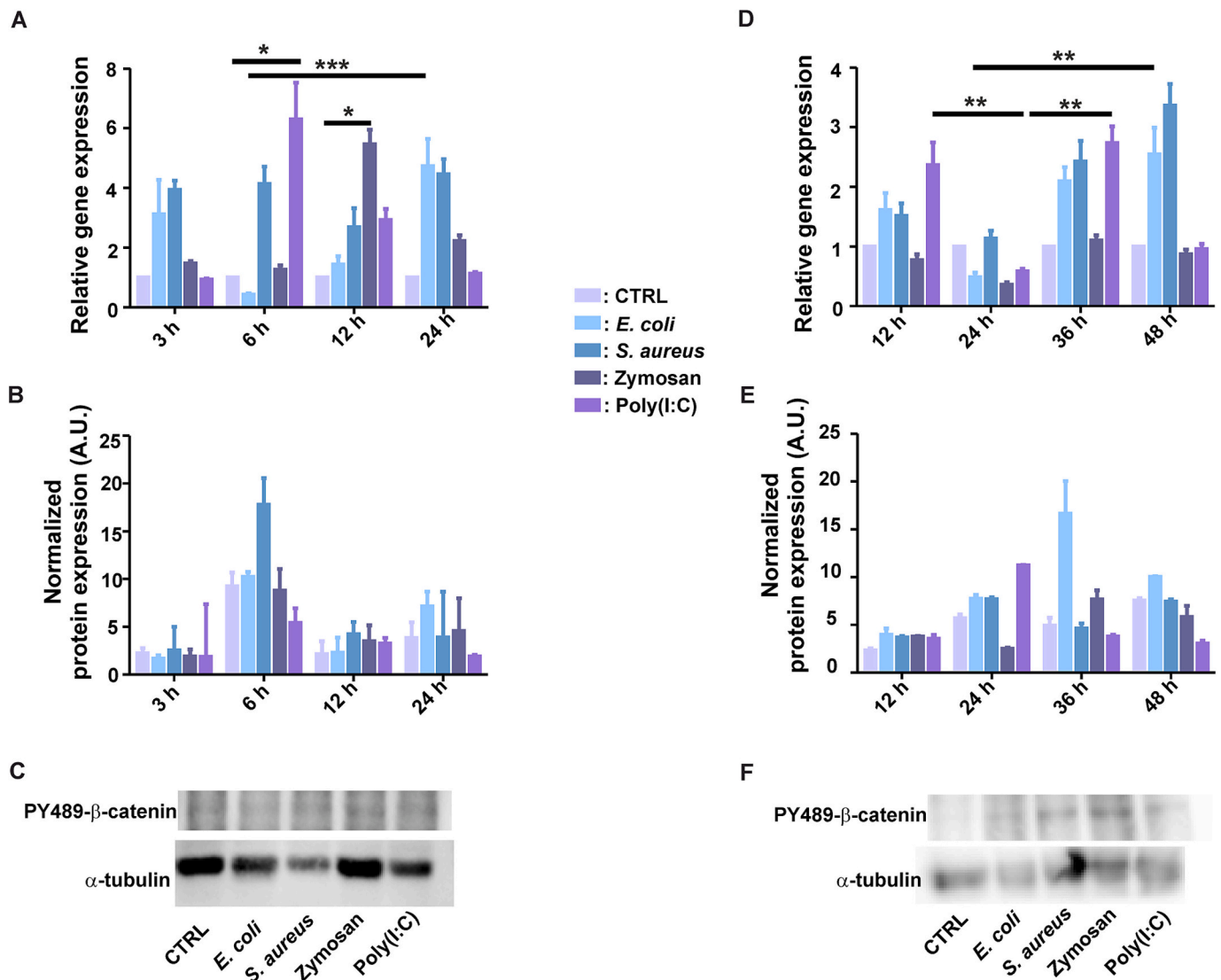


Fig. 7. Evaluation of *Ea-β-catenin* mRNA (A) and PY489-β-catenin protein (B) expression in *E. andrei* earthworm coelomocytes following *in vitro* microbial challenge measured by qPCR and Western blot, respectively. Representative example of Western blot experiment (C). Following *in vivo* microbial challenge *Ea-β-catenin* mRNA (D) and protein (E) expression were measured from *E. andrei* coelomocytes by qPCR and Western blot, respectively. Representative example of Western blot experiment (F). Mouse monoclonal anti-α-tubulin was applied as a loading control antibody in both *in vitro* and *in vivo* experiments. Bar graphs represent the mean ± SEM (qPCR, $n = 6$; Western blot, $n = 3$). Asterisks point out significant differences ($*p < 0.05$, $**p < 0.01$, $***p < 0.001$, Kruskal-Wallis).

anterior and posterior segment restoration, which was attenuated by the 4th week of restoration (Figs. 5, 6). This cell proliferation kinetics verifies our previous observation of the *E. andrei* tissue restoration process [27]. In addition, we noticed a characteristic difference in the amount of cells expressing *Ea-β-catenin* and mRNA expression regarding anterior or posterior regeneration. During anterior segment restoration, PY489-β-catenin-expressing cells were non-significantly increased, and *Ea-β-catenin* mRNA was significantly elevated in the regenerating blastema. In contrast, during posterior regeneration the number of PY489-β-catenin expressing cells dropped over time. Similarly, *Ea-β-catenin* mRNA expression decreased in the 2nd week and increased by the 4th week, but it was still significantly lower compared to intact animals (Figs. 5 and 6). To this end, *Ea-β-catenin* is involved with an assorted dynamic in both anterior and posterior regenerative morphogenesis of earthworms, similarly during the head and foot regeneration in *Hydra* [47].

Interestingly, various pathogen (viruses or bacteria strains) stimuli enhanced the β-catenin expression in several invertebrates [12,13,36,37] or vertebrate models [50–52]. Coelomocytes isolated from *E. andrei* earthworms and exposed *in vitro* to microbial stimuli have

shown variable *Ea-β-catenin* mRNA expressions. Zymosan and Poly(I:C) treatments (12 h and 6 h, respectively) significantly elevated the *Ea-β-catenin* mRNA expression levels (Fig. 7), while *in vivo* poly(I:C) stimuli had a significant, but transient effect on *Ea-β-catenin* mRNA. These results prove the involvement of β-catenin in invertebrate (including earthworms) innate immune response against microbial infections.

To validate the molecular interactions involved in the Wnt/β-catenin pathway, several cell-permeant small compounds can be applied [28]. In this regard, we chose LiCl and iCRT14 to target the binding partners of *E. andrei* β-catenin. With LiCl exposure, the molecular contact between GSK-3 and β-catenin is diminished, so consequently the Wnt/β-catenin signaling pathway is activated [53], while iCRT14 treatment inhibits the TCF/β-catenin interaction resulting in the inhibition of Wnt/β-catenin pathway [54]. Indeed, coelomocytes exposed *in vitro* to LiCl have showed elevated *Ea-β-catenin* mRNA levels (Fig. 8A) and induced nuclear translocation of PY489-β-catenin (Fig. 8C). In contrast, iCRT14 treatment caused attenuated expression of *Ea-β-catenin* mRNA (Fig. 8D) and PY489-β-catenin is more pronounced in the cytoplasm of coelomocytes (Fig. 8F). In this regard, our results support the notion of

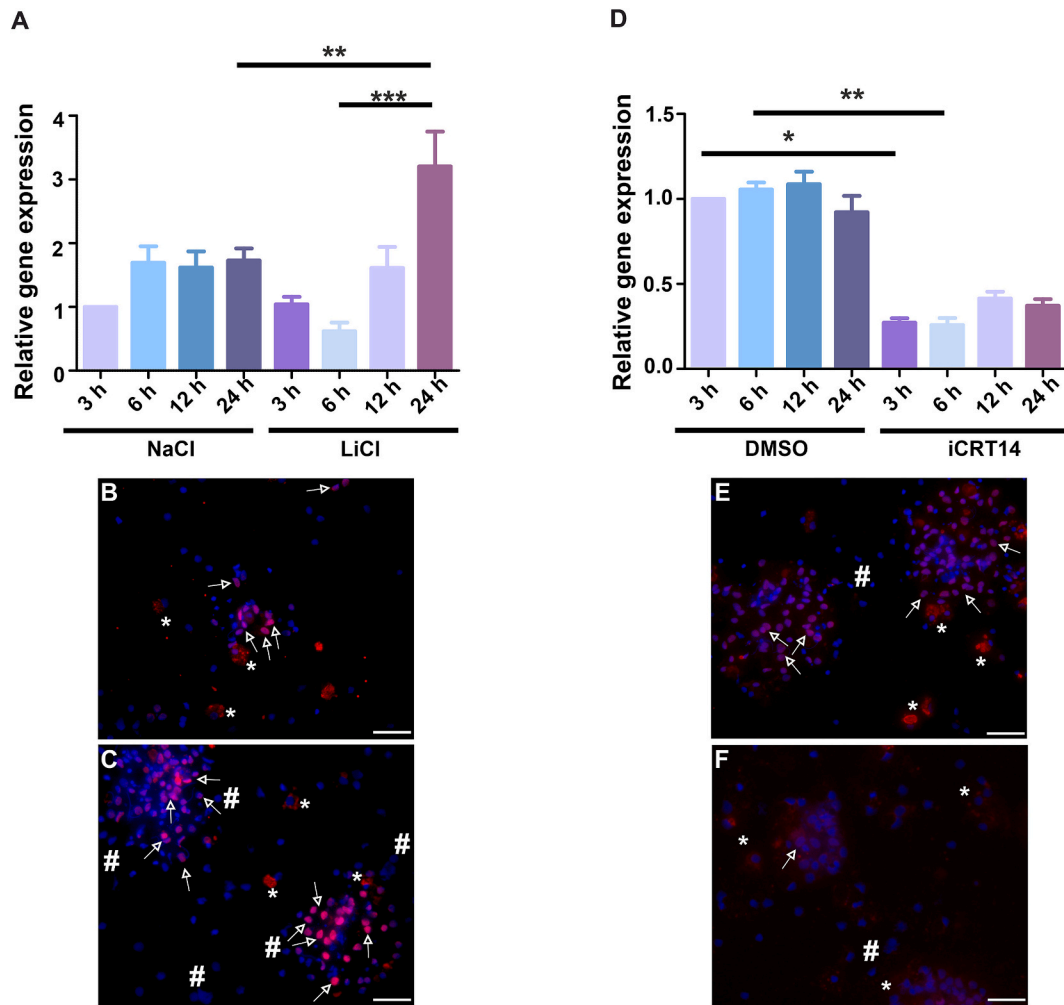


Fig. 8. *In vitro* induction of *Ea-β-catenin* mRNA expression in coelomocytes by LiCl (24 h) treatment (A). Decrease of *Ea-β-catenin* mRNA expression of coelomocytes upon *in vitro* iCRT14 treatment (D). Bar graphs depict the mean \pm SEM ($n = 6$). Asterisks designate significant differences ($*p < 0.05$, $**p < 0.01$, $***p < 0.001$, Kruskal-Wallis). Immunofluorescence localization of PY489- β -catenin protein in coelomocytes following 24 h exposure with NaCl (B), LiCl (C), DMSO (E), and iCRT14 (F) solutions. Note prominent nuclear translocations (white outlined arrows) of PY489- β -catenin (red), compared to cytoplasmic signal (asterisks). Negative cell clusters are marked with number sign. Nuclear counterstaining was performed with DAPI solution (blue). Scale bars: 200 μ m.

functional presence of *Ea-β-catenin* along with its binding partners, most importantly, GSK-3.

Our recent data regarding the identification and characterization of a novel member of the β -catenin family in annelid earthworms adds further information to its evolutionary conservation of structure and function. Furthermore, it strengthens the evidence of conservation of the canonical Wnt-signaling pathway in Lophotrochozoan invertebrates.

CRediT authorship contribution statement

Kornélia Bodó: Writing – original draft, Methodology, Investigation, Formal analysis, Conceptualization. **Ákos Boros:** Writing – review & editing, Methodology, Investigation. **Chayeen Brotzki da Costa:** Writing – review & editing, Investigation. **Gréta Tolnai:** Investigation. **Éva Rumppler:** Writing – review & editing, Investigation. **Zoltán László:** Investigation. **György Nagyri:** Writing – review & editing, Methodology, Investigation, Formal analysis. **Péter Németh:** Writing – review & editing, Resources. **Peter Kille:** Writing – review & editing, Resources. **László Molnár:** Writing – review & editing, Resources. **Péter Engelmann:** Writing – review & editing, Visualization, Methodology, Investigation, Funding acquisition, Formal analysis, Conceptualization.

Declaration of competing interest

The authors declare no conflict of interest.

Acknowledgements

This research was funded by the Medical School Research Foundation University of Pécs (KA-2022-03), University of Pécs (020_2024_PTE_RK/7, 020_2024_PTE_RK/36), EKÖP-24-4-II-PTE-130, GINOP-232-15-2016-00050, EFOP-361-16-2016-00004, National Brain Project (NAP2022-I-10/2022, BLRI), Laboratory of Water Science and Water Security (RRF 2.3.1-21-2022-00008, HUN-REN, BLRI). Project No. TKP2021-EGA-10 has been implemented with the support provided by the Ministry of Culture and Innovation of Hungary from the National Research, Development and Innovation Fund, financed under the TKP2021 funding scheme. The work was supported by the ÚNKP-19-3-I New National Excellence Program of the Ministry for Innovation and Technology, K.B.; and the János Bolyai Research Scholarship of the Hungarian Academy of Sciences, P.E. Á.B. was supported by the György Romhányi Research Scholarship of the University of Pécs, Medical School. We express our thanks to Soft-Flow Ltd. (Pécs, Hungary) allowing us to use the Olympus ScanR high-content screening station. We are thankful to Dániel Dunai (Faculty of Sciences, University of Pécs)

for providing earthworm specimens. We would like to acknowledge the help of Tamás Nagy, Dávid Szinger, and Dávid Ernszt (Medical School, Clinical Center, University of Pécs) and we appreciate the helpful discussion about the beta-catenin specific antibodies of Vitalij Kozin (St. Petersburg State University, Russia).

Appendix A. Supplementary data

Supplementary data to this article can be found online at <https://doi.org/10.1016/j.ijbiomac.2025.141397>.

References

- V.V. Kozin, I.E. Borisenko, R. Kostyuchenko, Establishment of the axial polarity and cell fate in metazoan via canonical Wnt signaling: new insights from sponges and annelids, *Biol. Bull.* 46 (2019) 14–25.
- Valenta, G. Hausmann, K. Basler, The many faces and functions of β -catenin, *EMBO J.* 31 (2012) 2714–2736.
- I.S. Gul, P. Hulpiau, Y. Saeyns, F. van Roy, Evolution and diversity of cadherins and catenins, *Exp. Cell Res.* 358 (2017) 3–9.
- J. Liu, B.T. Phillips, M.F. Amaya, J. Kimble, W. Xu, The C. elegans SYS-1 protein is a bona fide beta-catenin, *Dev. Cell* 14 (2008) 751–761.
- S.Q. Schneider, J.R. Finnerty, M.Q. Martindale, Protein evolution: structure-function relationships of the oncogene beta-catenin in the evolution of multicellular organisms, *J. Exp. Zool.* 295B (2003) 25–44.
- A. Marineau, K.A. Khan, M.J. Sevant, Roles of GSK-3 and β -catenin in antiviral innate immune sensing of nucleic acids, *Cells* 9 (2020) 897.
- E. Pascual-Carreras, M. Marin-Barba, S. Castillo-Lara, P. Coronel-Córdoba, M. S. Magri, G.N. Wheeler, J.L. Gómez-Skarmeta, J.F. Abril, E. Saló, T. Adell, Wnt/ β -catenin signalling is required for pole-specific chromatin remodelling during planarian regeneration, *Nature Comm.* 14 (2023) 298.
- A. Tursch, N. Bartsch, M. Mercker, J. Schlüter, M. Lommel, A. Marciniak-Czochra, S. Özbek, T.W. Holstein, Injury-induced MAPK activation triggers body axis formation in Hydra by default Wnt signaling, *Proc. Natl. Acad. Sci. U. S. A.* 119 (2022) e2204122119.
- A. Bertozzi, C.C. Wu, S. Hans, M. Brand, G. Weidinger, Wnt/ β -catenin signaling acts cell-autonomously to promote cardiomyocyte regeneration in the zebrafish heart, *Dev. Biol.* 481 (2022) 226–237.
- H. Yokoyama, H. Ogino, C.L. Stoick-Cooper, R.M. Grainger, R.T. Moon, Wnt/ β -catenin signaling has an essential role in the initiation of limb regeneration, *Dev. Biol.* 306 (2007) 170–178.
- O. Silva-García, J.J. Valdez-Alarcón, V.M. Baizabal-Aguirre, The Wnt/ β -catenin signaling pathway controls the inflammatory response in infections caused by pathogenic bacteria, *Mediators Inflamm.* 310183 (2014).
- J. Sun, L. Ruan, H. Shi, X. Xu, Characterization and function of a β -catenin homolog from *Litopenaeus vannamei* in WSSV infection, *Dev. Comp. Immunol.* 76 (2017) 412–419.
- G. Wang, F. Liu, J. Xu, J. Ge, J. Li, Identification of *Hc- β -catenin* in freshwater mussel *Hyriopsis cumingii* and its involvement in innate immunity and sex determination, *Fish Shellfish Immunol.* 91 (2019) 99–107.
- F.J.T. Staal, T.C. Luis, M.M. Tiemessen, WNT signalling in the immune system: WNT is spreading its wing, *Nat. Rev. Immunol.* 8 (2008) 581–593.
- M. Baril, S. Es-Saad, L. Chatel-Chaix, K. Fink, T. Pham, V.A. Raymond, K. Audette, A.S. Guenier, J. Duchaine, M. Servant, M. Bilodeau, E. Cohen, N. Grandvaux, D. Lamarre, Genome-wide RNAi screen reveals a new role of WNT/CTNBN1 signaling pathway as negative regulator of virus-induced innate immune response, *PLoS Path.* 9 (2013) e1003416.
- S.B. Cohen, N.L. Smith, C. McDougal, M. Pepper, S. Shah, G.S. Yap, H. Acha-Orbea, A. Jiang, B.E. Clausen, B.D. Rudd, E.Y. Denkers, Beta-catenin signaling drives differentiation and proinflammatory function of IRF8-dependent dendritic cells, *J. Immunol.* 194 (2015) 210–222.
- Y.K. Xie, D. Ding, H.M. Wang, C.J. Kang, A homologous gene of *β -catenin* participates in the development of shrimp and immune response to bacteria and viruses, *Fish Shellfish Immunol.* 47 (2015) 147–156.
- K.G. Nyberg, M.A. Conte, J.L. Kostyuk, A. Forde, A.E. Bely, Transcriptome characterization via 454 pyrosequencing of the annelid *Pristina leidyi*, an emerging model for studying the evolution of regeneration, *BMC Genomics* 13 (2012) 287.
- R.P. Ribeiro, G. Ponz-Segrelles, C. Bleidorn, M.T. Aguado, Comparative transcriptomics in Syllidae (Annelida) indicates that posterior regeneration and regular growth are comparable, while anterior regeneration is a distinct process, *BMC Genomics* 20 (2019) 855.
- L. Molnár, P. Engelmann, I. Somogyi, L.L. Mácsik, E. Pollák, Cold-stress induced formation of calcium and phosphorous rich chloragocyte granules (chloragosomes) in the earthworm, *Eisenia fetida*, *Comp. Biochem. Physiol.* 163A (2012) 199–209.
- K. Bodó, Á. Boros, É. Rumpel, L. Molnár, K. Böröcz, P. Németh, P. Engelmann, Identification of novel lumbricin homologues in *Eisenia andrei* earthworms, *Dev. Comp. Immunol.* 90 (2019) 41–46.
- Á. Boros, P. Pankovics, P. Simmonds, G. Reuter, Novel positive-sense, single stranded RNA (+ssRNA) virus with di-cistronic genome from intestinal content of freshwater carp (*Cyprinus carpio*), *PLoS One* 6 (2011) 0029145.
- Á. Boros, P. Pankovics, N.J. Knowles, G. Reuter, Natural interspecies recombinant bovine/porcine enterovirus in sheep, *J. Gen. Virol.* 93 (2012) 1941–1951.
- K. Okonechnikov, O. Golosova, M. Fursov, The UGene team. Unipro UGENE: a unified bioinformatics toolkit, *Bioinform* 28 (2012) 1166–1167.
- K. Tamura, G. Stecher, S. Kumar, MEGA11: molecular evolutionary genetics analysis version 11, *Mol. Biol. Evol.* 38 (2021) 3022–3027.
- Á. Boros, Z. Herbert, G. Kiszler, J. Németh, D. Reglődi, A. Lubics, P. Kiss, A. Tamás, S. Shioda, K. Matsuda, E. Pollák, L. Molnár, Changes in the PACAP-like compounds during the embryonic development of the earthworm *Eisenia fetida*, *J. Mol. Neurosci.* 36 (2008) 157–165.
- K. Bodó, Z. Kellermayer, Z. László, Á. Boros, B. Kokhanyuk, P. Németh, P. Engelmann, Injury-induced innate immune response during segment regeneration of the earthworm, *Eisenia Andrei*, *Int. J. Mol. Sci.* 22 (2021) 2363.
- S. Bello, V. Torres-Gutiérrez, E.J. Rodríguez-Flores, E.J. Toledo-Román, N. Rodríguez, L.M. Díaz-Díaz, L.D. Vázquez-Figueroa, J.M. Cuesta, V. Grillo-Alvarado, A. Amador, J. Ryes-Rivera, J.E. Garcia-Araraás, Insights into intestinal regeneration signaling mechanisms, *Dev. Biol.* 458 (2020) 12–31.
- P. Engelmann, Y. Hayashi, K. Bodó, D. Ernszt, I. Somogyi, A. Steib, J. Orbán, E. Pollák, P. Németh, L. Molnár, Phenotypic and functional characterization of coelomocyte subsets: linking light scatter-based cell typing and imaging of the sorted populations, *Dev. Comp. Immunol.* 65 (2016) 41–52.
- K. Bodó, D. Ernszt, P. Németh, P. Engelmann, Distinct immune-and defense-related molecular fingerprints in separated coelomocyte subsets of *Eisenia andrei* earthworms, *Inv. Surv. J.* 15 (2018) 338–345.
- H. Aberle, A. Bauer, J. Stappert, A. Kispert, R. Kemler, β -Catenin is a target for the ubiquitin-proteasome pathway, *EMBO J.* 16 (1997) 3797–3804.
- B.J. DuChez, C.L. Hueschen, S.P. Zimmerman, Y. Baumer, S. Wincovitch, M. P. Playford, Characterization of the interaction between β -catenin and sorting nexin 27: contribution of the type I PDZ-binding motif to Wnt signaling, *Biosci. Rep.* 39 (2019) BSR20191692.
- Z. Steinhart, S. Angers, Wnt signaling in development and tissue homeostasis, *Development* 145 (2018) dev146589.
- D.X. Liu, Z.F. Li, Y.S. Zhao, L.M. Wang, H.Y. Qi, Z. Zhao, F.Q. Tan, W.X. Yang, Es- β -catenin affects the hemolymph-testes barrier in *Eriocheir sinensis* by disrupting cell junctions and cytoskeleton, *Int. J. Biol. Macromol.* 242 (2023) 124867.
- S.Q. Schneider, B. Bowerman, β -Catenin asymmetries after all animal/vegetal-oriented cell division in *Platynereis dumerilii* embryos mediate binary cell-fate specification, *Develop.* Cell 13 (2007) 73–86.
- K.H. Chandramouli, J. Sun, F.S. Mok, L. Liu, J.W. Qiu, T. Ravasi, P.Y. Qian, Transcriptome and quantitative proteome analysis reveals molecular processes associated with larval metamorphosis in the polychaete *Pseudopolydora vexillosa*, *J. Proteome Res.* 12 (2013) 1344–1358.
- S. Zhang, L. Shi, K.L.H. Li, S. Wang, J. He, C. Li, Cloning, identification and functional analysis of a β -catenin homologue from Pacific white shrimp, *Litopenaeus vannamei*, *Fish Shellfish Immunol.* 54 (2016) 411–418.
- Z. Zhang, Z. Lv, W. Zhang, M. Luo, C. Li, A novel β -catenin from *Apostichopus japonicus* mediated *Vibrio splendidus*-induced inflammatory-like response, *Int. J. Biol. Macromol.* 156 (2020) 730–739.
- S.G. Tevosian, N.L. Manuylov, To beta or not to beta: canonical beta-catenin signaling pathway and ovarian development, *Dev. Dyn.* 237 (2008) 3672–3680.
- Y. Shi, W. Liu, M. He, Proteome and transcriptome analysis of ovary, intersex gonads, and testis reveals potential key sex reversal/differentiation genes and mechanism in scallop *Chlamys nobilis*, *Marine Biotechnol.* 20 (2018) 220–245.
- C. Santerre, P. Sourdaïne, B. Adeline, A.S. Martinez, Cg-SoxE and Cg- β -catenin, two new potential actors of the sex-determining pathway in a hermaphrodite lophotrochozoan the Pacific oyster, *Crassostrea gigas*, *Comp. Biochem. Physiol.* 167A (2014) 68–76.
- J.P. Lyons, R.K. Miller, X. Zhou, G. Weidinger, T. Deroo, T. Denayer, J.I. Park, H. Ji, J.Y. Hong, A. Li, R.T. Moon, E.A. Jones, K. Vlemmeckx, P.D. Vize, P.D. McCreia, Requirement of Wnt/beta-catenin signaling in pronephric kidney development, *Mech. Dev.* 126 (2009) 142–159.
- J. Schneider, A.A. Arraf, M. Grinstein, R. Yelin, T.M. Schultheiss, Wnt signalling orients the proximal-distal axis of chick kidney nephrons, *Development* 142 (2015) 2686–2695.
- J.S. Park, M.T. Valerius, A.P. McMahon, Wnt/beta-catenin signaling regulates nephron induction during mouse kidney development, *Development* 134 (2007) 2533–2539.
- D. Bastakoty, P.P. Young, WNT/ β -catenin pathway in tissue injury: roles in pathology and therapeutic opportunities for regeneration, *FASEB J.* 30 (2016) 3271–3284.
- V. Daponte, P. Tylzanowski, A. Forlino, Appendage regeneration in vertebrates: what makes that possible? *Cells* 10 (2021) 242.
- S. Guffer, B. Artes, H. Bielen, I. Krainer, M.K. Eder, J. Falschlunger, A. Bollmann, T. Ostermann, T. Valovka, M. Hartl, K. Bister, U. Technau, B. Hobmayer, β -Catenin acts in a position independent regeneration response in the simple eumetazoan *Hydra*, *Dev. Biol.* 433 (2018) 310–323.
- M. Sureda-Gómez, J.M. Martín-Durán, T. Adell, Localization of planarian β -catenin-1 reveals multiple roles during anterior-posterior regeneration and organogenesis, *Development* 143 (2016) 4149–4160.
- Y. Shao, X.B. Wang, J.J. Zhang, M.L. Li, S.S. Wu, X.Y. Ma, X. Wang, H.F. Zhao, Y. Li, H.H. Zhu, D.M. Irwin, D.P. Wang, G.J. Zhang, J. Ruan, D.D. Wu, Genome and single-cell RNA sequencing of the earthworm *Eisenia andrei* identifies cellular mechanisms underlying regeneration, *Nat. Commun.* 11 (2020) 2656.
- F. Binder, M. Hayakawa, M.K. Choo, Y. Sano, J.M. Park, Interleukin-4-induced β -catenin regulates the conversion of macrophages to multinucleated giant cells, *Mol. Immunol.* 54 (2013) 157–163.
- T.D.W. Kasthuriarachichi, J.C. Harasgama, S. Lee, H. Kwon, Q. Wan, J. Lee, Cytosolic β -catenin is involved in macrophage M2 activation and antiviral defense

- in teleosts: delineation through molecular characterization of β -catenin homolog from redlip mullet (*Planizia haematocheila*), Fish Shellfish Immunol. 118 (2021) 228–240.
- [52] L. Wu, J. Zhang, M. Wu, X. Zhao, X. Shi, W. Ma, X. Li, Y. Zhou, Roles of β -catenin in innate immune process and regulating flora in Qi river crucian carp (*Carassius auratus*), Fish Shellfish Immunol. 148 (2024) 109521.
- [53] P.S. Klein, D. Melton, A molecular mechanism for the effect of lithium on development, Proc. Natl. Acad. Sci. U. S. A. 93 (1996) 8455–8459.
- [54] F.C. Gonsalves, K. Klein, B.B. Carson, S. Katz, L.A. Ekas, S. Evans, An RNAi-based chemical genetic screen identifies three small molecule inhibitors of the Wnt/wingless signaling pathway, Proc. Natl. Acad. Sci. U. S. A. 108 (2011) 5954–5963.